



A robotic indenter for minimally invasive measurement and characterization of soft tissue response

Evren Samur, Mert Sedef, Cagatay Basdogan, Levent Avtan, Oktay Duzgun

► To cite this version:

Evren Samur, Mert Sedef, Cagatay Basdogan, Levent Avtan, Oktay Duzgun. A robotic indenter for minimally invasive measurement and characterization of soft tissue response. *Medical Image Analysis*, 2007, 11 (4), pp.361-373. 10.1016/j.media.2007.04.001 . hal-03177346

HAL Id: hal-03177346

<https://hal.science/hal-03177346>

Submitted on 23 Mar 2021

HAL is a multi-disciplinary open access archive for the deposit and dissemination of scientific research documents, whether they are published or not. The documents may come from teaching and research institutions in France or abroad, or from public or private research centers.

L'archive ouverte pluridisciplinaire **HAL**, est destinée au dépôt et à la diffusion de documents scientifiques de niveau recherche, publiés ou non, émanant des établissements d'enseignement et de recherche français ou étrangers, des laboratoires publics ou privés.

A Robotic Indenter for Minimally Invasive Measurement and Characterization of Soft Tissue Response

Evren Samur^a, Mert Sedef^a, Cagatay Basdogan^{a*}
Levent Avtan^b, Oktay Duzgun^c

^aCollege of Engineering, Koc University, Istanbul, Turkey

^bFaculty of General Surgery, Istanbul University, Istanbul, Turkey

^cFaculty of Veterinary Medicine, Istanbul University, Istanbul, Turkey

* Corresponding author:
Cagatay Basdogan, Ph.D.
College of Engineering
Koc University
Rumelifeneri yolu, Istanbul, 34450, Turkey
Tel: 90+ 212-338-1721
Fax: 90+ 212-338-1548
e-mail: cbasdogan@ku.edu.tr

Abstract

The lack of experimental data in current literature on material properties of soft tissues in living condition has been a significant obstacle in the development of realistic soft tissue models for virtual reality based surgical simulators used in medical training. A robotic indenter was developed for minimally invasive measurement of soft tissue properties in abdominal region during a laparoscopic surgery. Using the robotic indenter, force versus displacement and force versus time responses of pig liver under static and dynamic loading conditions were successfully measured to characterize its material properties **in three consecutive steps**. First, the effective elastic modulus of pig liver was estimated as 10-15 kPa from the force versus displacement data of static indentations based on the small deformation assumption. Then, the stress relaxation function, relating the variation of stress with respect to time, was determined from the force versus time response data via curve fitting. Finally, an inverse finite element solution was developed using ANSYS finite element package to estimate the optimum values of viscoelastic and nonlinear hyperelastic material properties of pig liver through iterations. The initial estimates of the material properties for the iterations were extracted from the experimental data for faster convergence of the solutions.

Keywords: robotic indenter, laparoscopic surgery, surgical simulation, minimally invasive measurement, soft tissue characterization, linear viscoelasticity, hyperelasticity, inverse finite element solution.

1. Introduction

The lack of data in current literature on material properties of soft tissues in living condition (in-vivo) and in natural position inside the body (in-situ) has been a significant obstacle in the development of virtual reality based surgical simulators that can provide the user with realistic visual and haptic feedback (Basdogan et al., 2004, Sedef et al., 2006). Most tissue characterization experiments conducted in the past have been mainly performed in laboratory conditions outside the living body (in-vitro). The experimental data has been collected from tissue samples of known geometries under well-defined loading and boundary conditions using standard mechanical testing devices (Fung, 1993). However, recent experimental studies report that mechanical properties of soft tissues obtained through in-vivo and in-situ measurements are different than the similar properties obtained through in-vitro measurements (Kauer, 2001, Brown et al., 2003, Ottensmeyer et al., 2004). Since the integration of incorrect material properties into deformable tissue models for simulating surgical procedures may result in adverse training effects, acquisition and characterization tissue properties in a living body is an important and necessary step towards the development of realistic surgical simulators.

Soft organ tissues exhibit complex nonlinear, anisotropic, nonhomogeneous, time, and rate dependent behavior, which are extremely challenging to measure and simulate. In this study, we present new approaches for the measurement of displacement and force responses of soft tissues using a robotic indenter to characterize their material properties. In comparison to the earlier measurement systems, our robotic measurement system is minimally invasive and designed to make large indentations on internal organs in the abdominal region during a laparoscopic surgery. Using the proposed system, two sets of animal experiments were conducted in an operating room to measure force-displacement and force-time responses of pig liver. An inverse finite element solution, utilizing an iterative optimization algorithm, was developed to estimate the hyperelastic and viscoelastic material properties of pig liver from the experimental data.

The following section provides necessary background and literature review related to the characterization of soft tissue behavior. The concepts of minimally invasive surgery are introduced

and the existing techniques for measurement of soft tissue response are reviewed. The design details of our robotic indenter are given in Section 3. In addition, the controller design and the preliminary experiments are discussed in Section 3. The experimental set-up and procedures are described in Section 4. The results of our animal experiments are also presented in this section. Section 5 presents the material properties of pig liver estimated from the experimental data. The inverse finite element solution is also discussed in this section. Finally, we conclude the study in Section 6 with a discussion of the performed work and the future research studies.

2. Literature Review

2.1. Minimally Invasive Surgery and Virtual Reality

Minimally Invasive Surgery (MIS) has been used increasingly for many surgical procedures over the last two decades. In this technology, surgeons use a small video camera connected to a video screen, and customized surgical tools to perform surgery with minimal injury to tissue. For example, in laparoscopy, the camera and instruments are inserted into abdominal cavity through small holes (**up to 2 cm**) on the skin allowing the surgeon to explore the cavity without the need of making large cuts as in open surgery. Major advantages of this type of surgery to the patient are short hospital stay, timely return to work, and less pain and scarring after the surgery.

Although these advantages make MIS widespread, there are some difficulties associated with the use of this technology as discussed in Basdogan et al. (2001). Training for laparoscopy is crucial and relies on simulated models, animals, and guidance from experienced surgeons in the operating room (OR). However, animal use is being reduced for ethical and cost reasons and guidance in the OR presents danger to the patient. The simulated models used for training can be grouped as mechanical models and virtual reality (VR) based models. In mechanical models, a simple box equipped with laparoscopic tools and a camera is used to operate on artificial objects and materials such as beads and rubber. Although this training method is easy to carry out, it has many drawbacks like unrealistic representation of organs and surgical environment. In VR based models on the other hand, surgical procedures are simulated in a multimodal virtual environment with visual and haptic feedback to

trainee. Although there are technical challenges in developing realistic simulations, VR is a promising technology for medical training (see the list of references in Basdogan et al., 2001, Basdogan et al., 2004, and Delingette and Ayache, 2004). The most significant challenge in VR-based surgical simulation is the development of realistic soft tissue models. To meet this challenge, material properties of soft tissues in a living condition and within the body must be obtained and integrated into the simulators for realistic training. Ottensmeyer et al. (2004) emphasize that if the tissue models or parameters are significantly different than reality, negative training transfer may result from the use of the flawed simulator. Furthermore, Brown et al. (2003) indicate that the knowledge of material properties would be useful not only to simulation, but also for optimizing surgical tool design, creating intelligent devices that are capable of assessing the pathology, and understanding the mechanism of tissue injury.

2.2 Measurement of Soft Tissue Properties

Soft organ tissues exhibit complex nonlinear, anisotropic, nonhomogeneous, time, and rate dependent behavior. Fung (1993) has revealed that nonlinear stress-strain relationship is common for soft tissues but the degrees are different for different tissues. Since soft organs are composed of different materials, like elastin and collagen, in different combinations, soft tissue properties are both coordinate and direction dependent. Time and rate dependent behavior is also common and explained by viscoelasticity.

Material properties of soft tissues are highly challenging to measure and several different methods have been proposed in the past (see Table 1). **These methods can be divided into two groups according to the measurement site as in-situ and in-vitro (or ex-vivo).** In-vitro or ex-vivo measurements are performed outside the body using standard material testing methods (i.e. tension or compression tests) under well-defined boundary conditions. Most tissue experiments conducted in the past have been in-vitro studies and the experimental data has been collected from the excised and well-shaped tissue samples. However, material properties of soft tissues change in time and the results obtained from in-vitro measurements can be misleading. Dead organ and muscle tissues typically stiffen with time. The results obtained by Ottensmeyer et al. (2004) show that measurement

environment of in-vitro studies does not represent the actual tissue conditions. For this reason, research in this area has been recently focused on measurement of mechanical properties of soft tissues in a living state (in-vivo) and with-in the body (in-situ) (Carter et al., 2001, Ottensmeyer, 2001, Kauer 2001, Tay et al., 2002, Brown et al., 2003, Samur et al., 2005).

The techniques for measuring mechanical properties of soft organ tissues can also be divided into three groups according to the degree of damage made to tissue during the measurements. In invasive methods, measurement is performed by entering into the body through puncture or large incisions. Because large openings allow insertion of test apparatus into the body easily, many measurements have been performed invasively (Carter et al., 2001, Brouwer et al., 2001, Tay et al., 2002). However, the experimental devices and procedures used for the invasive measurements do not typically match the actual surgical devices and procedures used during a minimally invasive surgery. Besides, the invasive approach is not ideal for conducting human experiments. On the contrary, non-invasive measurements can be performed without making any incisions on the skin. Most commonly, ultrasonography and MRI are used to characterize tissue properties (Gao et al., 1996, Yong-Ping and Mak 1996, Manduca et al., 2001, Han et al., 2003). **Most of the techniques in this category can determine the material properties in the linear range only (Ottensmeyer, 2001).** However, it is known that soft organ tissues exhibit nonlinear material characteristics. In minimally invasive approach, small incisions are made on the body and tissue damage is much less than that of the invasive method. A few groups have recently conducted minimally invasive animal and human experiments to characterize nonlinear and time-dependent material properties of soft tissues (Ottensmeyer, 2001, Kauer 2001, Brown et al., 2003, Samur et al., 2005). The approaches followed by the researchers to measure soft organ properties can be divided into two groups: The first group of measurements involves the use of a hand-held instrument equipped with position and force sensors. An operator holds the instrument and indents organ surface manually to measure displacement and force response (Carter et al., 2001, Kauer 2001). Carter et al. (2001) conducted ex-vivo experiments with pig liver and in-vivo experiments with human liver using a hand-held probe. They estimated the elastic modulus of pig liver as 490 kPa and human liver as 270 kPa. Kauer (2001) performed tissue aspiration experiments using a hand-held instrument and collected data from pig kidney and human

uteri. The second group of measurements involves the use of a robotic device for providing better controlled stimuli (Rosen et al. 1999, Ottensmeyer, 2001, Tay et al., 2002, Brown et al., 2003, Hu and Desai, 2004, Valtorta and Mazza, 2005, Samur et al., 2005). Rosen et al. (1999) designed a laparoscopic grasper equipped with strain gages and then conducted in-vivo and in-situ experiments with porcine liver to measure forces during grasping (Brown et al., 2003). Ottensmeyer (2001) designed a robotic indenter to measure mechanical properties of pig liver during a minimally invasive surgery. His probe can make small indentations in the range of $\pm 500\mu\text{m}$. He conducted in-vivo experiments and estimated the elastic modulus of pig liver as 10-15 kPa. Tay et al. (2002) used a commercial robotic arm to achieve greater indentation depths up to 8 mm. The force response of pig liver to displacement stimulus was measured invasively using a force sensor attached to the tip of the arm during an open surgery. Later, Kim (2003) analyzed the experimental data and estimated the elastic modulus of pig liver as 3-4 kPa. Hu and Desai (2004) developed a robotic device to perform compression tests and measured the force and displacement response of pig liver. They conducted in-vitro experiments with the liver samples taken from pigs and developed methods to estimate the local effective modulus and hyperelastic material properties from the experimental data. Valtorta and Mazza (2005) developed a torsional resonator and estimated the complex shear modulus of porcine liver around 40 kPa using the data collected from in-vitro experiments.

Table 1. The classification of tissue measurement techniques.

Tissue Damage	Measurement Site	
	<i>in-situ</i>	<i>in-vitro</i>
Non-invasive	<ul style="list-style-type: none"> •Gao et al. •Yong-Ping and Mak •Manduca et al. •Han et al. 	
Minimally invasive	<ul style="list-style-type: none"> •Brown, et al. •Ottensmeyer •Samur, et al. •Kauer 	
Invasive	<ul style="list-style-type: none"> •Carter, et al. •Tay, et al. & Kim •Brouwer, et al. 	<ul style="list-style-type: none"> •Brouwer, et al. •Hu and Desai •Valtorta and Mazza

■	Medical imaging technique
■	Machine-operated electro-mechanical device
■	Human-operated electro-mechanical device

The characterization of material properties from the experimental data collected from in-vitro measurements is a relatively easy task since the cross-section of tissue sample, its boundary conditions, and the direction of loading are mostly known in advance. However, an inverse solution must be formulated to determine the unknown material properties from the measured response if there is not sufficient information about the experimental conditions (Schnur and Zabaras, 1991, Kauer et al., 2002, Tonuk and Silver-Thorn 2003, Kim 2003, Samami and Plewes, 2004, Liu et al., 2004). For this purpose, a finite element model of the soft tissue is constructed and used in tandem with an optimization method to match the experimental data with the numerical solution through iterations.

3. Robotic Indenter

3.1. Design Considerations

One method to measure complex material behavior of soft tissues is to make mechanical indentations on tissue and record force response with respect to indentation depth and elapsed time for further analysis. As discussed in Section 2, there are currently two forms of measuring soft tissue response during a minimally invasive surgery: a) free-form measurements and b) robotic measurements, which are both considered as possible candidates for our design. A “free-form” measurement typically involves the use of a hand-held probe equipped with position and force sensors. Major benefit of using a hand-held probe over a robotic arm is safety. Since the operator manually derives the probe, unexpected and risky movements are unlikely to happen. However, there are two problems with this design. First, the measurements are made manually and not repeatable. Carter et al. used a load-cell triggered by the operator to make more controlled indentations, which provides a partial solution to the repeatability problem (Carter et al., 2001). The second difficulty is the identification of a reference point for the displacement measurements. Linear Variable Differential Transformers (LVDTs) have been used as position sensors for relative measurement of tissue

displacement with respect to a reference point. However, it is not easy to keep the probe stationary during the measurements and hence the reference point changes as the probe moves.

On the other hand, if a robotic arm is used for the measurements, the problems related to the actuation and position sensing can be solved. More controlled indentations can be performed on tissue surface by a pre-programmed robotic arm and an indenter attached to the arm. In addition, a robotic arm can be programmed to generate different types of stimuli. Thus, dependency to a user is eliminated and repeatability is achieved. Besides, the tip coordinates of the indenter can be acquired using encoders of the robotic arm with respect to the fixed coordinate frame.

Other issues that must be considered in the measurement of live tissue properties inside the body are sterilization, safety, and compatibility with MIS. Sterilization of instruments in hospitals is carried out using steam under pressure, liquid or gaseous chemicals, or dry heat. Steam and ethylene oxide (gaseous) sterilization are performed at temperatures around 130°C and 50°C, respectively. On the other hand, liquid sterilization is performed at room temperature but takes longer time. Most of the standard sterilization techniques can easily damage the components of a robotic measurement system since its sensors and actuators are typically sensitive to heat and humidity. Therefore, the design must enable the parts to be easily assembled and disassembled for sterilization. Safety is another important concern. A motion control algorithm must be implemented to make indentations on tissue such that unexpected and risky movements must be avoided to prevent damaging tissue. A robotic system must shut down itself automatically if anomalies are detected. In addition, the indenter tip must be rounded to prevent damaging tissue during measurements.

Finally, the measurement system must be designed such that the data can be collected during a MIS. The indenter must be compatible with the surgical tools used in MIS and pass through standard surgical trocars (instruments that allow passage of surgical tools). Also, friction between the indenter and the trocar during measurements must be reduced to eliminate measurement errors.

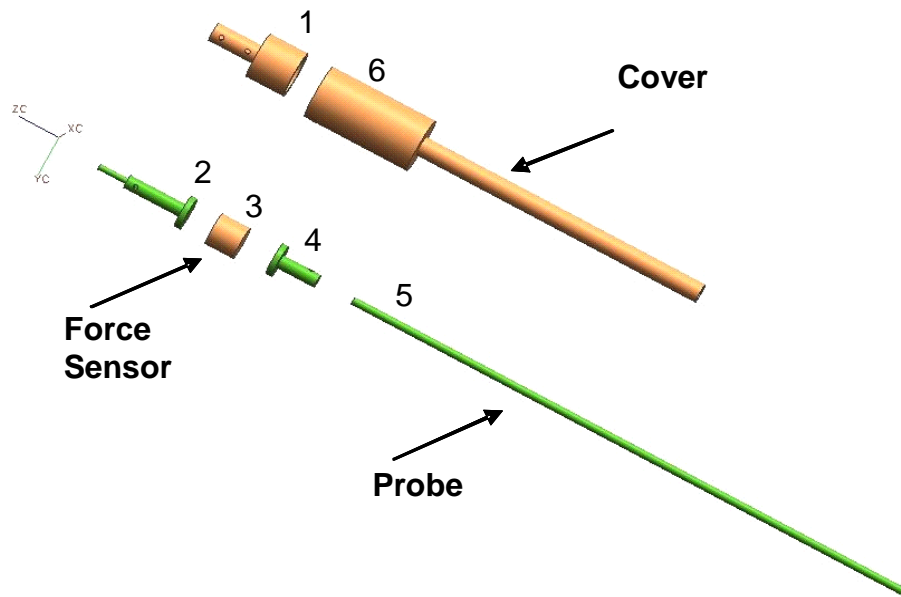
3.2. Design Details

Based on the design requirements discussed above, we have developed a robotic indenter to measure the material properties of soft tissues in the abdominal region during a MIS (Samur et al., 2005). The major components of our system include a robotic arm which can be programmed to make indentations on tissue, a long laparoscopic indenter which can be inserted into abdominal region through a surgical port, and a force sensor attached to the indenter for the measurement of force response of the tissue (Fig. 1). Using this system, we can make large indentations on internal organs in the abdominal region up to 10 mm. The robotic arm can be programmed to make cyclic indentations or indentations along a user-defined straight path with a given velocity. We used the Phantom haptic device (Model 1.0 from Sensable Technologies Inc.) as our robotic manipulator due to its versatility in position and velocity control in 3D space. The Phantom haptic device has a 13 x 18 x 25 mm workspace and a nominal position resolution of 0.03 mm. **The resonant frequencies of the device for x, y and z axes are 90 Hz, 60 Hz and 65 Hz, respectively (Cavusoglu et al., 2002).**

To access the internal organs in the abdominal region during a laparoscopic surgery, a special purpose indenter was designed. The indenter is rigidly attached to the haptic device and can be easily assembled and disassembled for sterilization. Also, the friction between the trocar and the indenter is eliminated. The indenter consists of two major parts: a laparoscopic probe fitted with a force/torque sensor and a cylindrical cover. Both parts are made of light-weight aluminum and separable into their sub-components for sterilization. The assembly order is given in Fig. 1b. The laparoscopic probe is a long solid shaft, having a diameter of 4 mm, with a round tip. A force-torque transducer (Nano 17 from ATI Industrial Automation Inc.) is used for the purpose of measuring force response. The Nano 17 has a force range of ± 50 N in the x and y directions and ± 70 N in the z direction and has a resolution of 1/1280 N along each of the three orthogonal axes when attached to a 16-bit A/D converter. **The resonant frequency for each degree of freedom is 7200 Hz.** Data acquisition unit includes a 16-bit analog input card PCI-6034E (National Instruments) with a maximum sampling rate of 200 kSamples/s.



(a)



(b)

Fig. 1. Our robotic indenter (a) and its components (b). The indenter is inserted into the abdominal cavity through a surgical trocar for collecting displacement and force data. The cover prevents the probe and force transducer from contacting the trocar during indentations. The numbers in the figure indicate the assembly order for sterilization purposes.

The cylindrical cover (see Fig. 1b) is a hollow shaft with two stages: the diameter of the first stage is sufficiently large enough to prevent the cover passing through a standard surgical trocar and the outer diameter of the second stage is small enough (10 mm) to insert the laparoscopic probe through the trocar. The major role of the cover is to prevent the laparoscopic probe and the force sensor

making contact with the trocar during measurements so that the friction between them does not introduce any errors in measurements.

3.3. Controller Design and GUI

A motion control algorithm must be implemented to make indentations on tissue surface. Using the software library of the Phantom haptic device and its position encoders, position of the end-effector point can be acquired in 3D space and appropriate torque commands can be sent to the actuators to control its motion. Using a PID controller, the tip point can be programmed to follow a straight line path with a specified rate. The proper selection of controller gains (i.e. PID tuning) is important for stable output response and the minimization of the steady-state error. We tuned our controller gains on six different material samples having varying softness before the animal experiments. This process enabled us to construct a look-up table for the feasible set of controller gains to be used in animal experiments.

We also developed a graphical user interface (GUI) to record current time, displacement, and force data in a text file following each experiment. The GUI was developed in MS Visual C++ environment using an ActiveX component to acquire force values from the force sensor attached to the indenter and the position values from the encoders of the robotic arm at 1 kHz. Using the GUI and the controller, static and dynamic stimuli can be generated easily. Using the GUI, the values of stimulus parameters such as pre-indentation depth, rate of indentation, final indentation depth, and stimulation time can be entered.

4. Animal Experiments

4.1. Experimental Procedures

We conducted animal experiments in collaboration with medical staff from Istanbul University, Department of Surgery (Faculty of Medicine) and Faculty of Veterinary Medicine in an operating room (Fig. 2). The experimental set-up and protocol were approved by a committee for use on animals. The indentation experiments were conducted with three adult pigs to characterize the

material properties of their liver. **The preparation of the measurement system in the operating room, which mainly involves the connection of the robotic device to the computer and the assembly of the indenter (Fig. 1), took less than 10 minutes.**



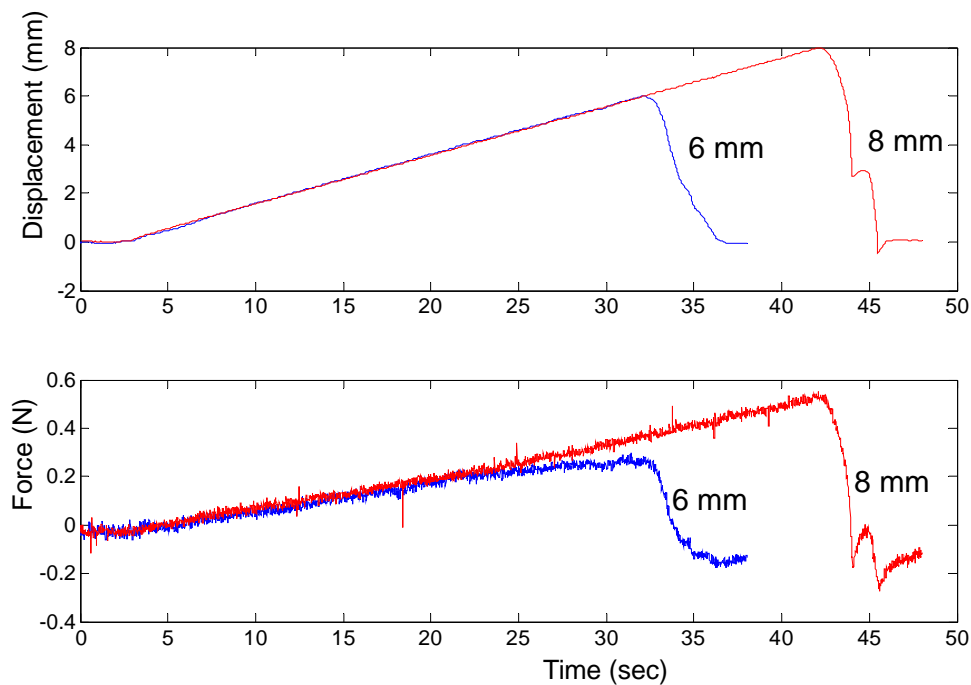
Fig. 2. A scene from the animal experiments.

Following the administration of anesthetic drugs, an incision was made in the abdominal area of each pig to insert a surgical trocar and then to inflate the abdominal cavity with carbon dioxide gas in order to have a larger working space and a better vision of the cavity. Two additional trocars were placed on the abdominal wall to insert a small video camera and the laparoscopic indenter. Using an adjustable table and the camera, the orientation of the indenter were adjusted to be perpendicular to the liver surface. We initially observed that breathing of the animal causes movements of the organs and abdominal wall which adversely affected the measured data. For this reason, each animal was euthanized before the data collection and all data was collected in one hour post-mortem. Brown et al. (2003) report no differences in elastic response of porcine liver within 3 hours post-mortem, but some difference was observed in the stress relaxation behavior. Before the data collection stage, liver of each pig was preconditioned with the same cyclic stimulus, having a pre-indentation depth of 3 mm, peak-to-peak amplitude of 3 mm, and a frequency of 0.1 Hz, for 60 seconds. After the preconditioning, static indentation and stress relaxation experiments were performed at the same site.

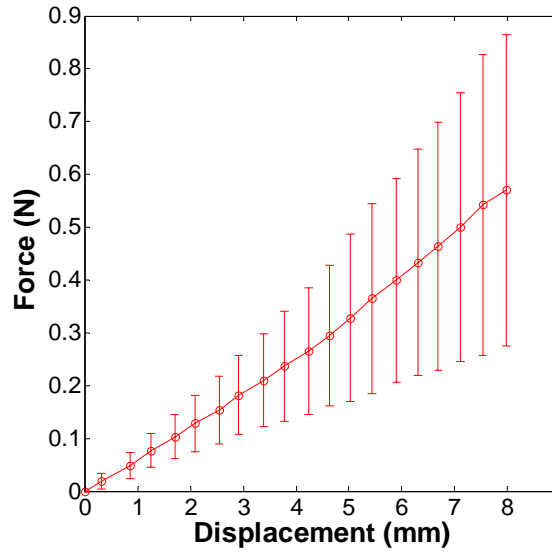
4.2. Indentation Experiments and Experimental Results

4.2.1. Static Indentation

In static loading, the liver of each pig was indented slowly from zero to the depths of 2, 4, 6, and 8 mm separately at a rate of 0.2 mm/s to characterize its force versus displacement response. Hence, a total of four measurements was taken from each pig. The raw displacement and force data collected from the liver of pig #2 as a function of time are shown in Fig. 3a. The average force response of 3 pigs for the indentation depth changing from zero to 8 mm is shown in Fig. 3b. As shown in the figure, the force response of pig liver shows more variation and nonlinearity as the penetration depth increases.



(a)



(b)

Fig. 3. a) The displacement-time and force-time curves constructed from the static indentation data of pig #2 for the indentation depths varying from zero to 6 and 8 mm with a strain rate of 0.2 mm/s. b) The average force response of 3 pigs for the indentation depth changing from zero to 8 mm with a strain rate of 0.2 mm/s.

4.2.2. Stress Relaxation

In stress relaxation experiments, the liver of each pig was first indented to pre-defined depths of 2, 4, 5, 6, and 8 mm in one second in separate trials and then the indenter was held there for 30 seconds to record the force relaxation response with respect to time. Hence, a total of four probing measurements was taken from each pig. The raw data collected from the liver of pig # 2 for different indentation depths is shown in Fig. 4a. The average response of three pigs at the indentation depth of 4 mm is shown in Fig. 4b.

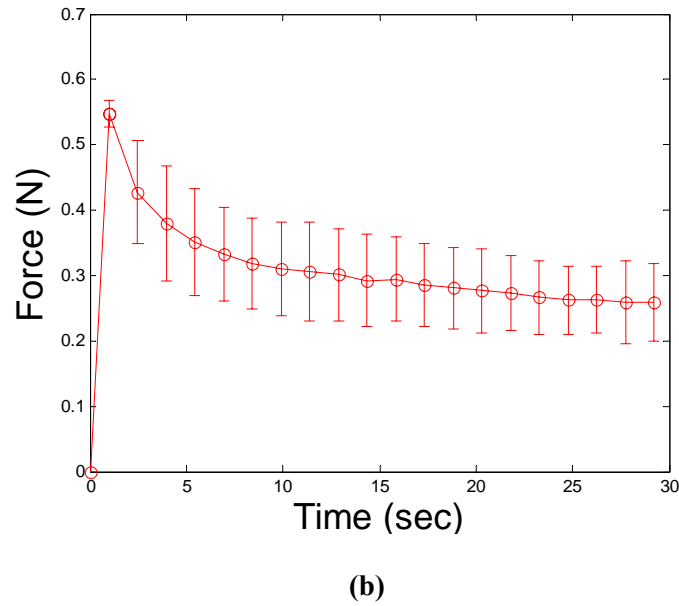
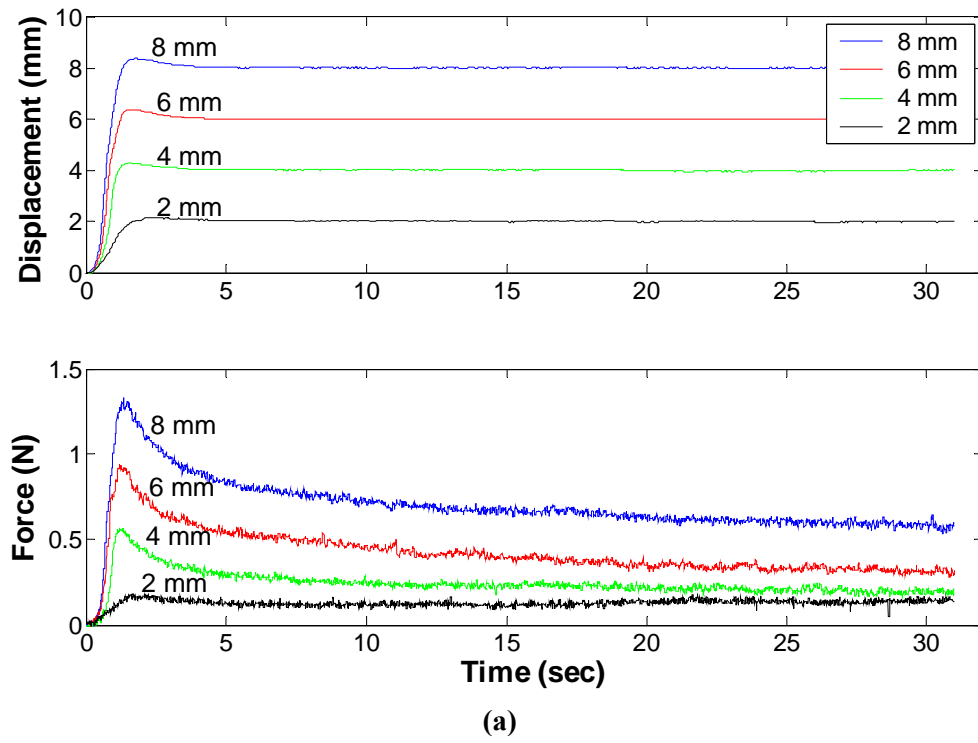


Fig. 4. a) The displacement-time and force-time curves generated from the raw stress relaxation data of pig #2 for the indentation depths of 2, 4, 6, and 8 mm (strain rates are 2, 4, 6, and 8 mm/s respectively). b) The average force-time response of 3 pigs at the indentation depth of 4 mm (strain rate is 4 mm/s). The data points represent the mean values of three animals and the vertical bars correspond to the standard deviations over one trial per animal.

5. Characterization of Material Properties

5.1. Linear Static Response

An effective shear and elastic moduli of pig liver was estimated from the static indentation data using the linear elastic contact theory and the small deformation assumption. The effective shear modulus, G , for small indentation of an elastic half-space by a rigid hemispherical indenter can be obtained using the solution given by Lee and Radok (1960):

$$G = \frac{3F}{16\delta\sqrt{R\delta}} \quad (1)$$

where, F is the force, δ is the indentation depth of a rigid sphere with a radius of R . From the relation between shear and elastic moduli for isotropic materials, effective elastic modulus, E , can be calculated:

$$E = 2G(1 + \nu) \quad (2)$$

where, ν is Poisson ratio and equal to 0.5 for incompressible materials. Using the Equations 1 and 2, the effective elastic modulus of pig liver was estimated from the experimental static indentation data for the different indentation depths (Table 2).

Table 2. The effective elastic modulus of pig liver calculated for the different indentation depths.

Indentation Depth δ [mm]	Effective Young's Modulus E [kPa]
2	16.9 ± 4.9
4	12.4 ± 4.1
6	10.8 ± 4.7
8	10.0 ± 4.7

5.2. Viscoelastic Response

The history of the stress response of viscoelastic materials was characterized by shear relaxation function $G(t)$, which can be represented by the Prony series (Gefen and Margulies, 2004) as

$$G(t) = G_{\infty} + \sum_{k=1}^N G_k e^{-t/\tau_k} \quad (3)$$

where, G_{∞} is the long-term shear modulus and G_k and τ_k are the coefficients of the Prony series. The coefficients of the Prony series for $N = 2$ were calculated via curve fitting (see Table 3) to the shear relaxation response, $G(t)$, which was obtained from the experimental force relaxation data using the small deformation assumption (Eq. 1).

Table 3. The coefficients of the shear relaxation function for the indentation depth of 4 mm.

	Pig #1	Pig #2	Pig #3
G_1 [kPa]	2.402	3.688	0.827
G_2 [kPa]	1.733	2.495	3.333
τ_1 [s]	0.979	1.000	1.202
τ_2 [s]	5.650	9.000	10.641
G_{∞} [kPa]	4.593	3.193	5.093

Fig. 5 shows the variation of the shear relaxation function of pig #2 with respect to time for the different indentation depths. As shown in the figure, the relaxation curves for different loadings almost overlap with each other, which is an indication of linear viscoelastic response (Haddad, 1995).

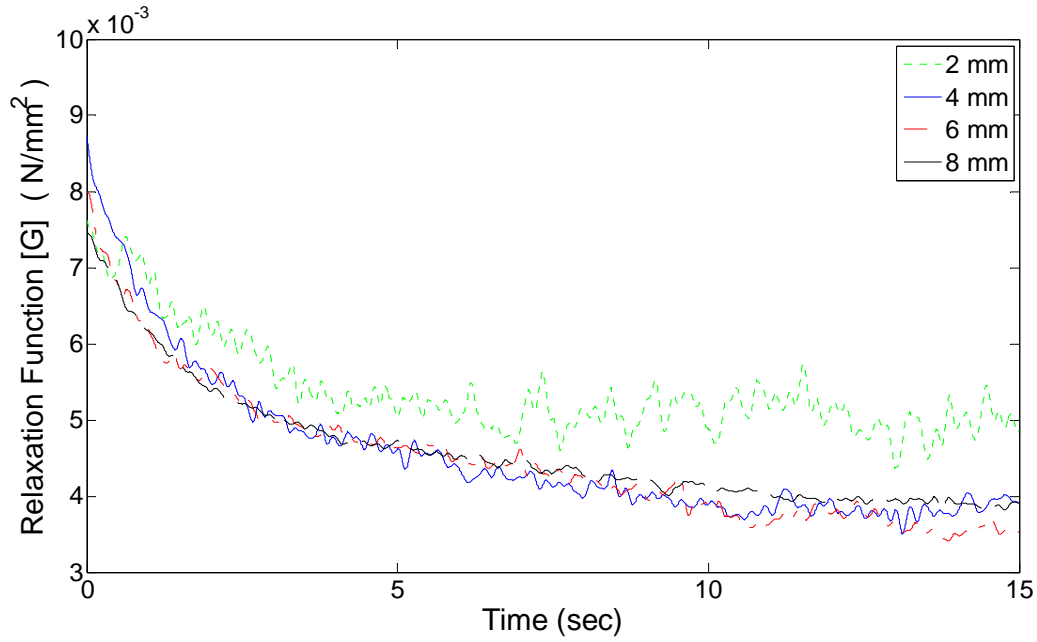


Fig. 5. The shear relaxation modulus of pig liver (pig #2) as a function of time for the different indentation depths and rates.

5.3. Inverse Finite Element Solution

The characterization of material properties based on experimental data is considered as the inverse problem. We used a finite element modeling package (ANSYS) and its optimization toolbox to solve the inverse problem. To develop the inverse solution, a finite element model of the liver was developed. The liver tissue around the contact region was modeled **as a semi-infinite elastic half space** using 2D axisymmetric finite elements (PLANE183) having hyperelastic, viscoelastic, large deflection, and large strain capabilities. **The material properties of the model were initially assumed to be homogeneous, isotropic, and nearly incompressible (the Poisson's ratio was set to 0.49).** The base and the lateral parts of the model were constrained to have no displacements. **The elastic modulus of the model was set to an approximate value of 15 kPa based on the results of the static indentation experiments (see Table 2).**

The finite element model of the indenter was constructed from the same type of 2D linear finite elements. The indenter was assumed to be rigid and its elastic modulus was set to a high value of 2 GPa. The ratio of the indenter radius to the height of the tissue model was set to a

value of 0.1 to approximate the semi-infinite elastic half space. A frictionless contact between the rigid indenter and the tissue model was assumed. To eliminate the effect of geometry on the small indentation calculations, the model was first indented to a depth of 2 mm and then the geometric size of the FEM model was slowly increased until the relative error in force response was less than a pre-determined threshold value of five percent. In addition, mesh density of the model was adjusted to reduce the total number of finite elements in the model for computational efficiency. For this purpose, we first started with a very fine mesh and then the elements which were not in the close proximity of the contact region and having little effect on the calculations were slowly enlarged until the relative error in force response exceeded the threshold value of five percent. As a result, an adaptive grid structure with an optimum number of interface elements was achieved.

After obtaining an optimum geometry and mesh density for the model, a sensitivity analysis was carried out to check the accuracy of the frictionless contact model. Contact is a highly nonlinear phenomenon and the contact stiffness (FKN in ANSYS) is the most important parameter affecting the accuracy and convergence of the finite element solution in contact analysis. The optimum value generating a converged solution with an acceptable level of accuracy is often problem dependent. The penetration tolerance factor (FTOLN in ANSYS) is another factor which affects the accuracy and convergence of the solution. The values of FKN and FTOLN were determined through iterations based on the same error criterion of less than 5 % relative error in force response.

Following these adjustments, we upgraded the model to account for material and geometric nonlinearities and viscoelastic effects. Hyperelastic behavior of liver was modeled using 2-term Mooney-Rivlin strain-energy function, W , as

$$W = C_{10}(I_1 - 3) + C_{01}(I_2 - 3) \quad (4)$$

where, C_{ij} are the material stiffness constants corresponding to elastic modulus in linear material and I_i are the principle invariants of the right Cauchy deformation tensor (Miller, 2000, Kauer et al., 2002, Kim 2003, Hu and Desai, 2004, Samani and Plewes, 2004).

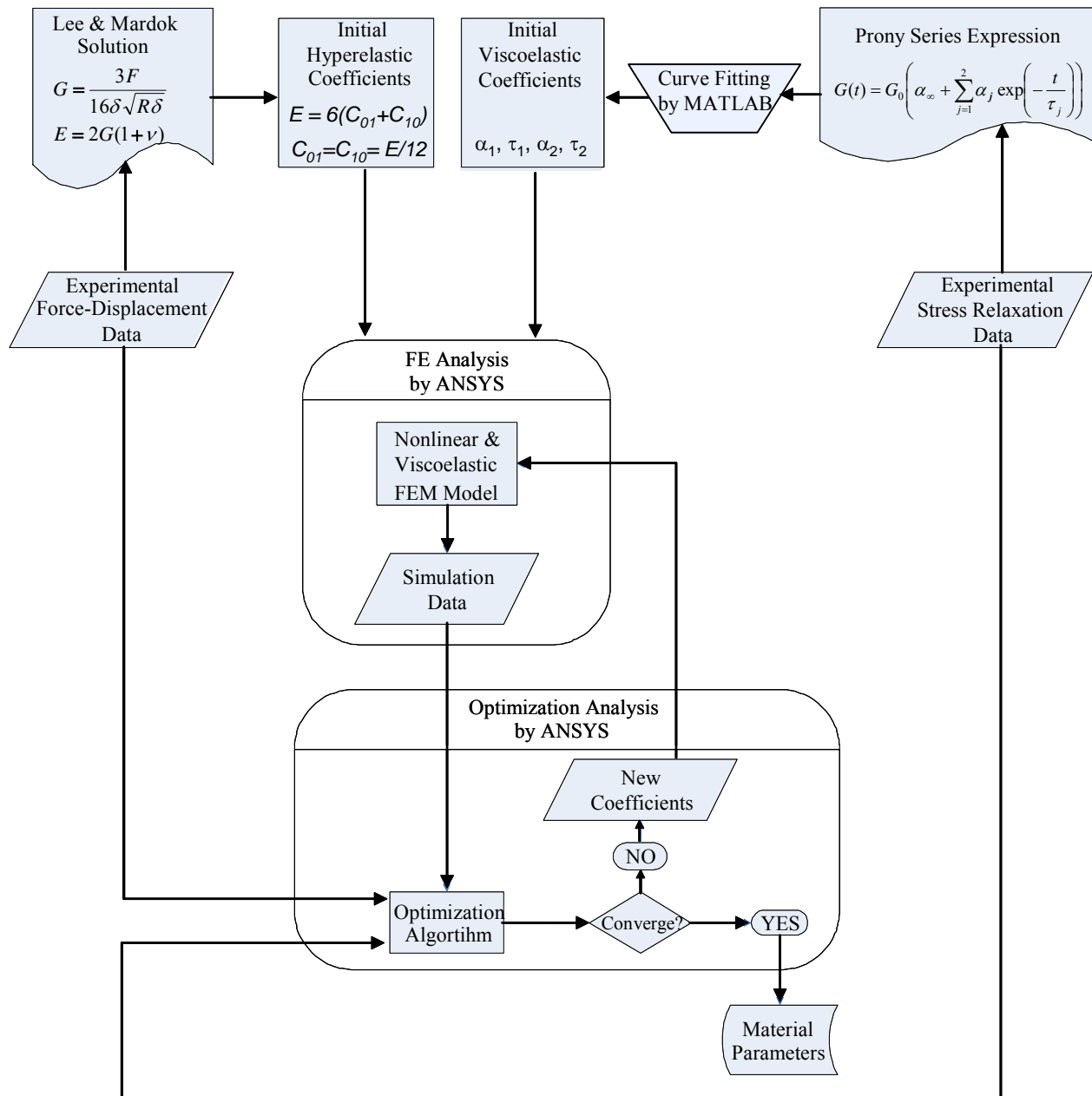


Fig. 6. The flow chart of the inverse finite element solution.

The viscoelastic behavior of liver was modeled using Prony series expansion having two terms. The viscoelastic formulation given in Eq. 3 is written for the long-term response of the stress relaxation function, but ANSYS uses the short-term representation of the same function which can be written for $N = 2$ as

$$G(t) = G_0 \left[\alpha_\infty + \sum_{k=1}^2 \alpha_k e^{-t/\tau_k} \right] \quad (5)$$

where, the coefficients τ_1 and τ_2 are the same as in Eq. 3 and $\alpha_\infty = G_\infty/G_0$, $\alpha_1 = G_1/G_0$, and $\alpha_2 = G_2/G_0$ are the relative moduli. G_0 is the short-term shear modulus (i.e. initial modulus) defined as $G_0 = G_\infty / (1 - \sum_{k=1}^2 \alpha_k)$.

The hyperelastic material coefficients, C_{10} and C_{01} as well as the viscoelastic material coefficients, α_1 , τ_1 , α_2 , and τ_2 were determined via the inverse solution through optimization iterations in ANSYS. The optimization algorithm minimizes the objective function defined as

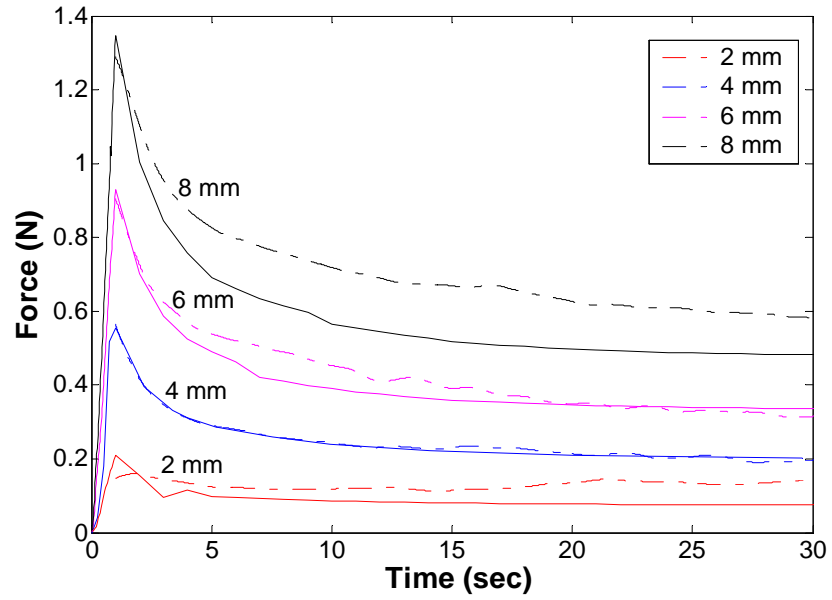
$$Error = \sum_{j=1}^M (F_j^{EXP} - F_j^{FEM})^2 \quad (6)$$

where, M represents the number of data samples, F_j^{EXP} is the experimental force value of the j^{th} sample, and F_j^{FEM} is the force value obtained from the FEM solution at the corresponding time step. The solution was iterated until the magnitude of error was less than or equal to 0.01 N. The initial estimates of hyperelastic coefficients, C_{10} and C_{01} , used in the iterations were determined by setting them equal to each other in the relation between the effective elastic modulus and Mooney-Rivlin constants for incompressible materials under infinitesimal strain conditions (Samani and Plewes, 2004) defined as $E = 6(C_{10} + C_{01})$. The viscoelastic coefficients calculated from the experimental stress relaxation data (Table 3) were used as the initial estimates of α_1 , τ_1 , α_2 , and τ_2 . The flow chart of

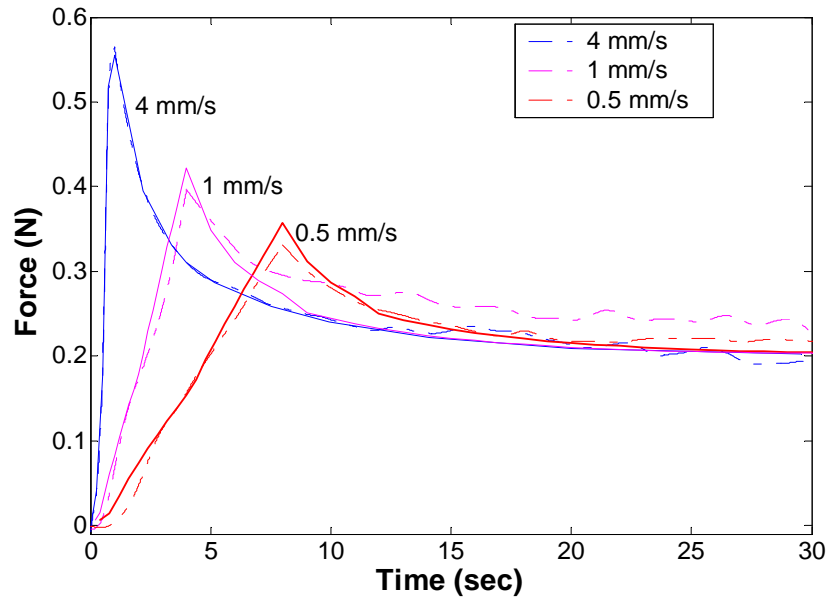
the optimization process is given in Fig. 6 and the material properties of three pigs estimated from the inverse solution are given in Table 4. The results of the inverse solution and the experimental data are compared in Figs. 7, 8, and 9.

Table 4. The estimated material properties of pig liver through inverse solution; α_k and τ_k are the viscoelastic coefficients and C_{01} and C_{10} are the hyperelastic coefficients. The hyperelastic coefficients given in the table correspond to the short-term response of the material. For conversion to the long-term response, they must be multiplied by $\left(1 - \sum_{k=1}^2 \alpha_k\right)$.

	Pig #1		Pig #2		Pig #3	
	Initial Value	Estimated Value	Initial Value	Estimated Value	Initial Value	Estimated Value
α_1	0.275	0.309	0.393	0.429	0.089	0.388
α_2	0.199	0.243	0.266	0.256	0.360	0.098
τ_1 [s]	0.979	0.945	1.000	1.033	1.202	2.992
τ_2 [s]	5.650	7.792	9.000	6.431	10.641	11.941
C_{01} [kPa]	3.484	3.295	3.426	2.779	2.120	2.876
C_{10} [kPa]	3.484	2.563	3.426	3.459	2.120	3.240
Iterations	29		18		36	
Error	3.764E-03		0.428E-03		3.462E-03	



(a)



(b)

Fig. 7. a) The experimental force relaxation curve recorded at the indentation depths of 2, 4, 6, and 8 mm (dashed lines) and the corresponding inverse FEM solution (pig #2). b) The experimental force relaxation curve recorded at the indentation depth of 4 mm at strain rates of 4, 1, and 0.5 mm/s (dashed lines) and the corresponding inverse FEM solution (pig #2).

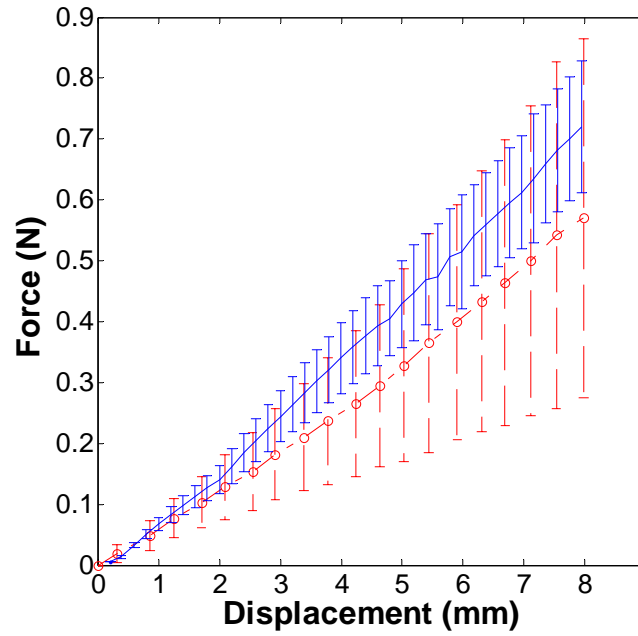


Fig. 8. The experimental force-displacement response of three pigs for the indentation depth of ranging from zero to 8 mm (red dashed line) and the corresponding forward FEM solution (blue solid line).

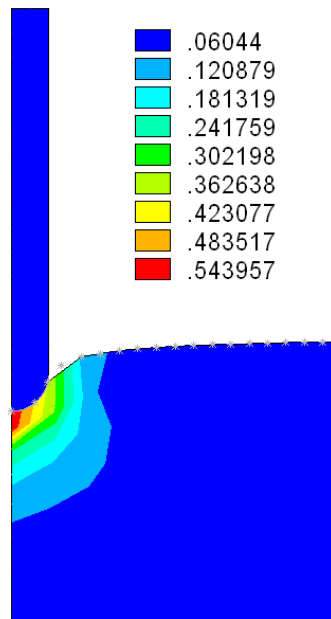


Fig. 9. The FEM analysis shows the distribution of maximum principal strain at the indentation depth of 4 mm (pig #2). Large deformations in the soft tissue (i.e. max principal strain \square max = 0.54) are observed around the contact region.

6. Discussion and Conclusion

We designed a robotic indenter for minimally invasive measurement of material properties of soft tissues. Using the indenter, animal experiments were conducted and force-displacement and force-time responses of pig liver were successfully measured under static and dynamic (rate-dependent) loading conditions. **Before the data collection, liver of each pig was preconditioned under cyclic loading. We observed that the preconditioning reduced the effect of hysteresis.** In comparison to the measurement systems developed in the past, our robotic measurement system is minimally invasive and designed to apply controlled stimulus to internal organs in the abdominal region during a laparoscopic surgery. In addition, most of the earlier measurement systems have relied on hand-held probes or can make small indentations only. An inverse finite element solution was developed for the characterization of material properties of pig liver from the experimental data. Characterization of tissue properties from the experimental data of in-situ measurements is a highly challenging task. Since the thickness and cross-sectional area of internal organs are not easy to measure, strain and stress values cannot be obtained directly from the measured displacement and force data. In our methodology, we estimate the viscoelastic and nonlinear hyperelastic material properties of pig liver from the experimental data in three steps. First, the effective elastic modulus of the liver was estimated as 10-15 kPa from the force-displacement data of static indentations using the small indentation assumption. A supporting value of 10-15 kPa was also reported by Ottensmeyer (2001). Then, the stress relaxation response of pig liver was modeled using Prony series and the coefficients of the model were determined via curve fitting to the experimental data. We observed that the stress relaxation curves of pig liver for different loading rates almost overlap with each other which is an indication of linear viscoelastic response (Fig. 5). Here, we should note that the stress relaxation function estimated from the experimental data must be interpreted with caution for two reasons. First, it was obtained based on the small deformation assumption. Second, the cut-off time for data recording (30 seconds in our experiments) affects its limiting value (Fung, 1993). As a final step, the optimum values of viscoelastic and nonlinear hyperelastic material properties were determined using

an inverse solution through iterations. To implement the inverse solution, a FEM model of liver tissue was constructed from axisymmetric 2D finite elements having homogeneous, isotropic, hyperelastic, viscoelastic, and nearly incompressible material properties. The hyperelastic behavior of liver was modeled using Mooney-Rivlin strain-energy function and the viscoelastic behavior was modeled using Prony series having two-terms. **The Mooney-Rivlin strain-energy function is sufficiently capable of representing nonlinear behavior and has computational advantages over the other models, which is critical for the real-time applications such as surgical simulation. Ogden and Arruda-Boyce strain functions have been also used by the biomechanics community to model nonlinear tissue behavior, but there is no clear consensus on which model is the best.**

The initial estimates of hyperelastic and viscoelastic material coefficients used in the iterations were obtained by processing the experimental data of static indentation and stress relaxation experiments (see the flow chart in Fig. 6). The results show that the viscoelastic coefficients estimated by the inverse solution are slightly different than the ones obtained from the experimental data via curve fitting. We believe that the difference originates from the fact that the Prony series was fit to the relaxation portion of the experimental data only as if the input is an ideal step displacement and also the small indentation solution of Lee and Radok's deviates from the actual response as the indentation depth increases. The material coefficients estimated through the inverse solution were used to perform a forward analysis in ANSYS to validate the results. **First, the principal strains are calculated to check if FEM model can actually display large deformations in the forward analysis (Fig. 9).** Then, the data generated by the forward solution was compared with the corresponding experimental data. The force versus time response generated by the forward ANSYS solution shows a good agreement with the corresponding experimental stress-relaxation data (Fig. 7). The force versus displacement solution obtained by the forward ANSYS analysis also shows a reasonable agreement with the corresponding experimental static indentation data for small indentations (Fig. 8). **The ANSYS solution slightly deviates from the experimental data as the indentation depth increases. However, the simulated force curves of three pigs are still in the range of experimental data (the inter-subject variation is approximately 0.1 N and the intra-subject variability over trials is 0.05 N).**

We should emphasize that there is a significant variation in the material properties of pig liver reported in the literature. One possible cause of this variation is the difference between measurement techniques. Delingette and Ayache (2004) argue that the rich perfusion of the liver affects its rheology and it is questionable if ex-vivo experiments can really access the material properties of actual liver tissue even if special care is taken to prevent the swelling or drying of the tissue. The recent experiments conducted by Ottensmeyer et al. (2004) also show the differences in material properties of pig liver as a function of time. **On the other hand, data obtained from in-vivo experiments should also be interpreted with caution since tissue response is location and direction dependent. For example, pig liver has six lobes with varying thicknesses and different layers which make its material properties non-homogeneous.** In addition, the assumptions made about the organ geometry, stress distribution, contact mechanics, and boundary conditions affect the estimation of material properties obtained through the inverse solution (Kauer, 2001). It is also known that the tissue properties vary within the same species and also between the different species.

While the number of studies on in-vivo measurement of animal organ properties is increasing, there are only a few experiments conducted with human subjects (Carter et al., 2001, Kauer 2001). In both studies, the experiments have been performed during an open surgery using hand-held probes. We paid special attention to sterilization, safety, and compatibility with minimally invasive surgery in our design to conduct human experiments in the future. Although we have successfully collected data from three pigs, there are still some problems to be solved in order to conduct human experiments. **First of all, the inverse solution including the measurement system must be fully validated with different material samples of known properties.** In addition, the stress relaxation experiments require long term loading of soft tissue that lasts for several seconds. It is obvious that long-term loading is not feasible in human experiments since assisted ventilation can be used for only short periods of time. The biomechanics literature suggests that cyclic loading can also be used to extract viscoelastic tissue properties in which the data can be collected for a shorter period of time (Lakes, 1998).

References

Basdogan, C., De, S., Kim, J., Muniyandi, M., Srinivasan, M.A., 2004. Haptics in minimally invasive surgical simulation and training. *IEEE Computer Graphics and Applications*. Vol. 24, No.2, pp. 56-64.

Basdogan, C. Ho, C., Srinivasan, M.A., 2001. Virtual environments for medical training: Graphical and haptic simulation of common bile duct exploration. *IEEE/ASME Transactions on Mechatronics*. Vol. 6, No. 3, pp. 267-285.

Brouwer, I., Ustin, J., Bentley, L., Sherman, A., Dhruv, N., Tendick, F., 2001. Measuring in vivo animal soft tissue properties for haptic modeling in surgical simulation. *Proc. MMVR Conference* pp 69-71.

Brown, J.D., Rosen, J., Kim, Y.S., Chang, L., Sinanan, M.N., Hannaford, B., 2003. In-vivo and in-situ compressive properties of porcine abdominal soft tissues, *Medicine Meets Virtual Reality*, Vol. 94, pp. 26-32.

Carter, F.J., Frank, T.G., Davies, P.J., McLean, D., Cuschier, A., 2001. Measurements and modeling of the compliance of human and porcine organs. *Medical Image Analysis*, Vol. 5, pp 231-236.

Cavusoglu, M.C., Feygin, D., Tendick, F., 2002. A critical study of the mechanical and electrical properties of the PHANTOM haptic interface and improvements for high-performance control. *Presence: Teleoperators and Virtual Environments*, Vol. 11:6, pp. 555-568.

Delingette, H., Ayache, N., 2004. Soft tissue modeling for surgery simulation. *Computational Models for the Human Body: Handbook of Numerical Analysis*, Ed: N. Ayache, Elsevier.

Findley, W.N., Lai, J.S., Onaran, K., 1976. Creep and relaxation of nonlinear viscoelastic materials. New York, Dover.

Fung, Y.C., 1993. Biomechanics: Mechanical properties of living tissues. 2nd ed. New York, Springer-Verlag.

Gao L., Parker, K.J., Lerner, R.M., Levinson, S.F., 1996. Imaging of the elastic properties of tissue: a review. *Ultrasound Med. Biol.* 22, pp. 959–977.

Gefen, A., Margulies, S.S., 2004. Are in vivo and in situ brain tissues mechanically similar?. *Journal of Biomechanics*, Vol. 37, pp. 1339-1352.

Haddad, Y.M., 1995, *Viscoelasticity of Engineering Materials*, London, Chapman & Hall.

Han, L., Noble, J.A., Burcher, M., 2003. A novel ultrasound indentation system for measuring biomechanical properties of in vivo soft tissue. *Ultrasound in Med. & Biol.*, Vol. 29, pp 813-823.

Hu, T., Desai, J.P., 2004. Characterization of Soft-Tissue Material Properties: Large Deformation Analysis. *Proceedings of International Symposium on Medical Simulation*, (Lecture Notes in Computer Science LNCS 3078), pp. 28-37, Cambridge, MA, June 17-18.

Kauer, M., 20001. Inverse finite element characterization of soft tissues with aspiration experiments. Ph.D. Thesis, Institute of Mechanical Systems, Diss No: 14233, ETH.

Kauer, M., Vuskovic, V., Dual, J., Szekely, G., Bajka, M., 2002. Inverse finite element characterization of soft tissues. *Medical Image Analysis*, Vol. 6, pp 275-287.

Kim, J., 2003. Virtual environments for medical training: Graphical and haptic simulation of tool-tissue Interactions. Ph.D. Thesis, Dept. of Mechanical Engineering, MIT.

Lakes, R., 1998. Viscoelastic solids. CRC Press.

Lee, E.H., Radok, J.R.M., 1960. The contact problem for viscoelastic bodies. *Journal of Applied Mechanics*, Vol. 27, pp. 438–444.

Liu, Y., Kerdok, A.E., Howe, R.D., 2004. A nonlinear finite element model of soft tissue indentation. *Proceedings of International Symposium on Medical Simulation*, (Lecture Notes in Computer Science LNCS 3078), pp 67-76, Cambridge, MA, June 17-18.

Manduca, A., Oliphant, T.E., Dresner, M.A., Mahowald, J.L., Kruse, S.A., Amromin, E., Felmlee, J.P., Greenleaf, J.F., Ehman, R.L., 2001, Magnetic resonance elastography: Non-invasive mapping of tissue elasticity, *Medical Image Analysis*, Vol. 5, pp. 237–254

Miller, K., 2000. Constitutive modeling of abdominal organs. *Journal of Biomechanics*, Vol. 33, pp. 367-373.

Ottensmeyer, M.P., 2001. Minimally invasive instrument for in vivo measurement of solid organ mechanical impedance. Ph.D. Thesis, Dept. of Mechanical Engineering, MIT.

Ottensmeyer, M.P., Kerdok, A.E., Howe, R.D., Dawson, S.L., 2004. The effects of testing environment on the viscoelastic properties of soft tissues. *Proc. of International Symposium on Medical Simulation*, pp. 9-18.

Rosen, J., Hannaford, B., MacFarlane, M.P., Sinanan, M.N., 1999. Force controlled and teleoperated endoscopic grasper for minimally invasive surgery-experimental performance evaluation. *IEEE Transactions on Biomedical Engineering*, Vol. 46, pp. 1212-1221.

Samani, A., Plewes, D., 2004. A method to measure the hyperelastic parameters of ex vivo breast tissue samples. *Phys. Med. Biol.*, Vol. 49, pp 4395-4405.

Samur, E., Sedef, M., Basdogan, C., Avtan, L., Duzgun, O., 2005. A Robotic Indenter for Minimally Invasive Characterization of Soft Tissues. *Proceedings of the 19th International Conference on Computer Assisted Radiology and Surgery*, Vol. 1281 , pp. 713-718 , June, Berlin.

Sedef, M., Samur, E., Basdogan, C., 2006, Real-time Finite-Element Simulation of Linear Viscoelastic Tissue Behavior Based on Experimental Data. *IEEE Computer Graphics and Applications*, Vol. 26, No. 5, pp. 58-68.

Schnur, D.S., Zabaras, N., 1991. An inverse method for determining elastic material properties and a material interface. *International Journal for Numerical Methods in Engineering*, Vol. 33, pp 2039-2057.

Tay, B.K., Stylopoulos, N., De, S., Rattner, D.W., Srinivisan, M.A., 2002. Measurement of in-vivo force response of intra-abdominal soft tissues for surgical simulation. *Proc. MMVR Conference* pp 514-519.

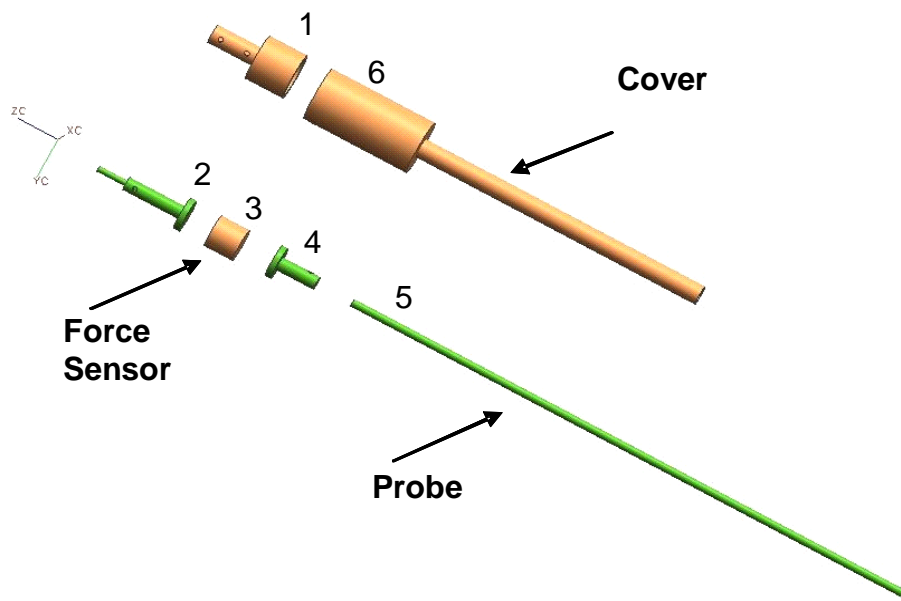
Tönük, E., Silver-Thorn, M.B., 2003. Nonlinear elastic material property estimation of lower extremity residual limb tissue. *IEEE Transactions on Neural Systems and Rehabilitation Engineering*, Vol. 11, pp 43-53.

Valtorta, D., Mazza, E., 2005. Dynamic measurement of soft tissue viscoelastic properties with a torsional resonator device, *Medical Image Analysis*, Vol. 9, No. 5, pp. 481-490.

Yong-Ping, Z., Mak, A.F., 1996. An ultrasound indentation system for biomechanical properties assessment of soft tissues in-vivo. *IEEE Transactions on Biomedical Engineering*, Vol. 43, pp. 912-918.



(a)

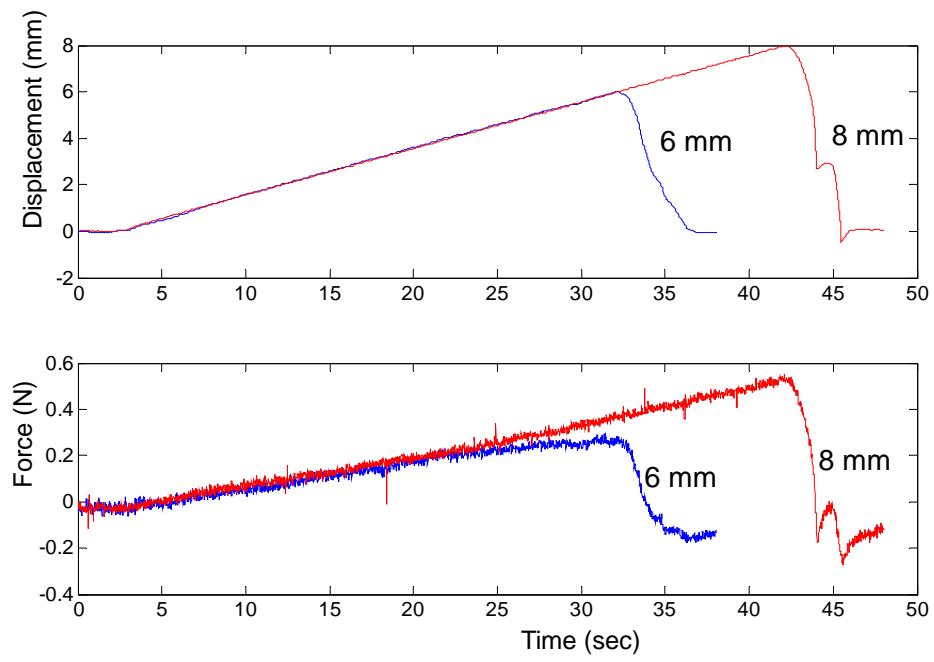


(b)

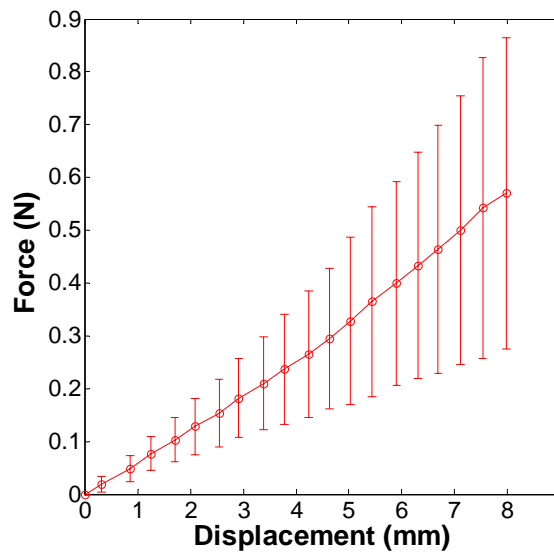
Figure 1.



Figure 2.



(a)



(b)

Figure 3.

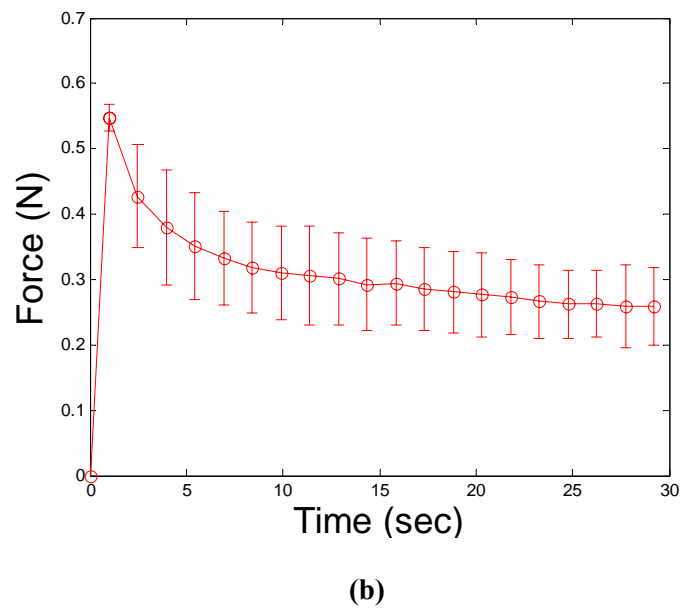
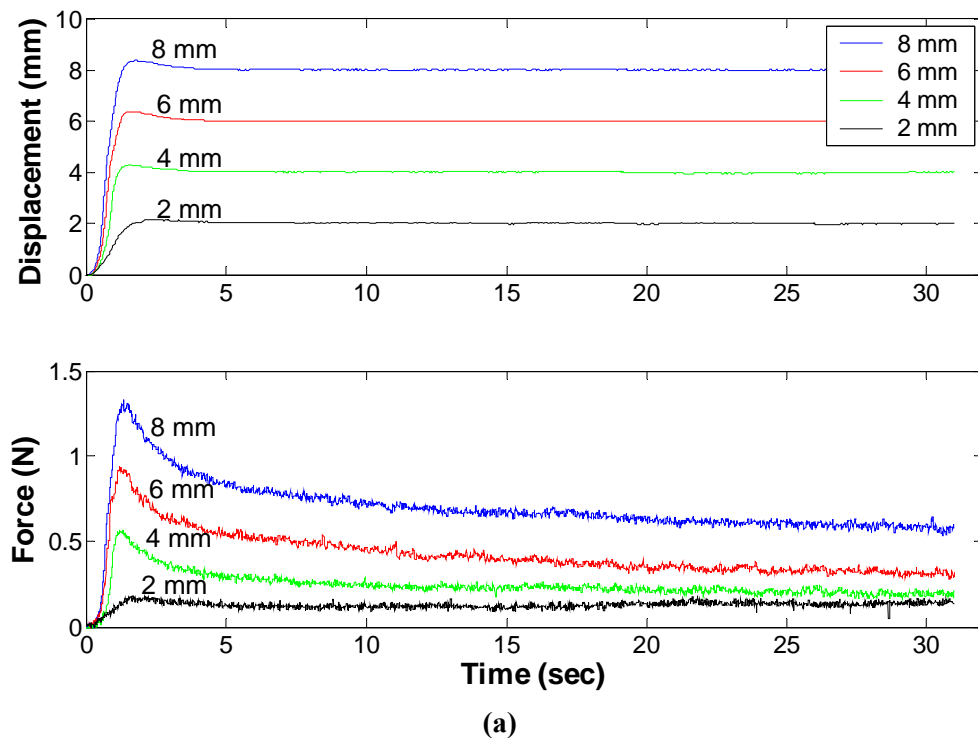


Figure 4.

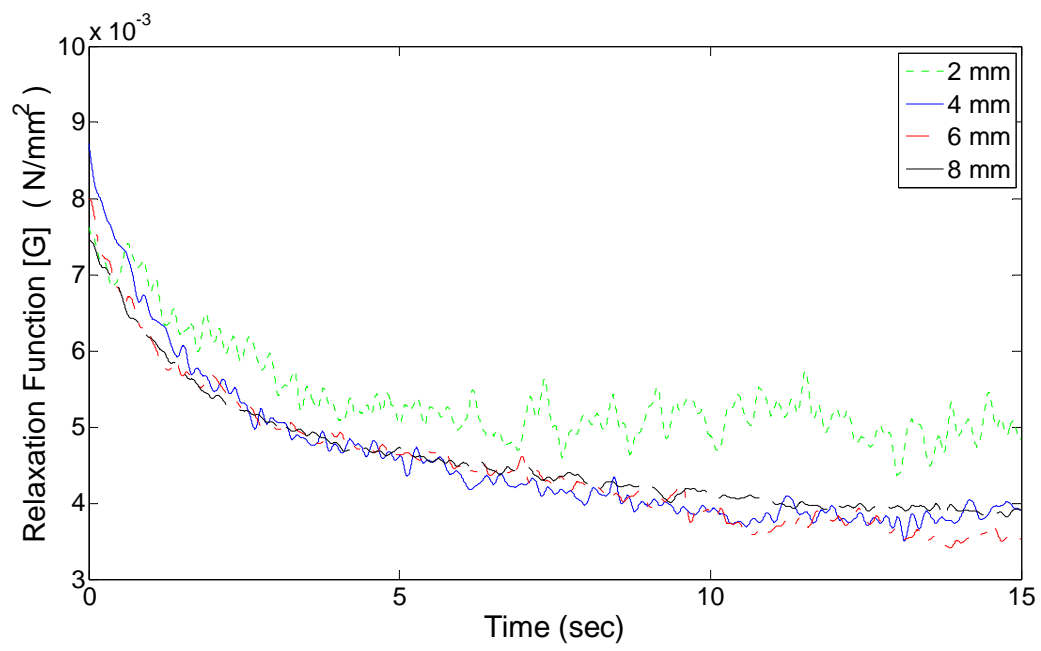


Figure 5.

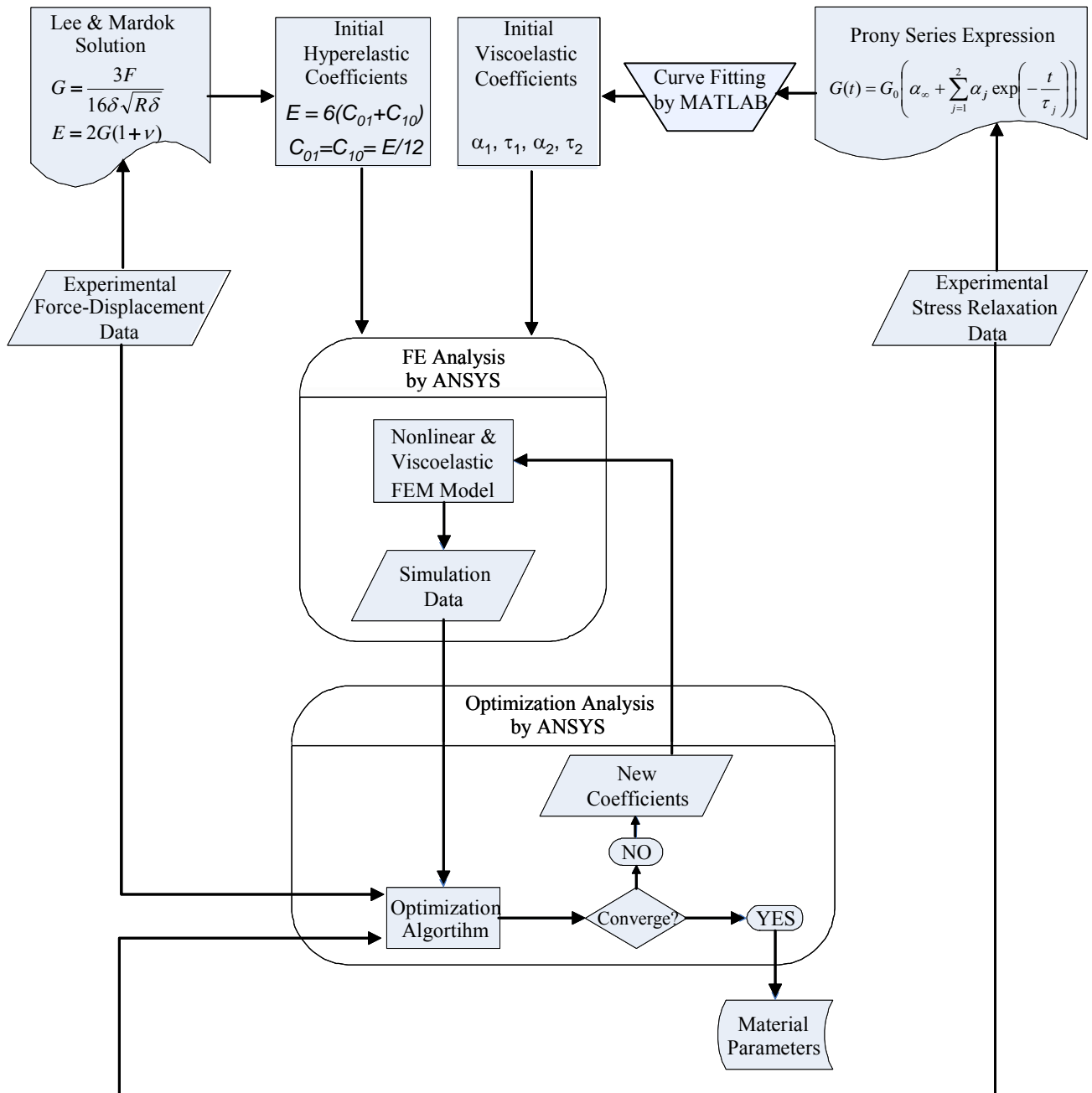
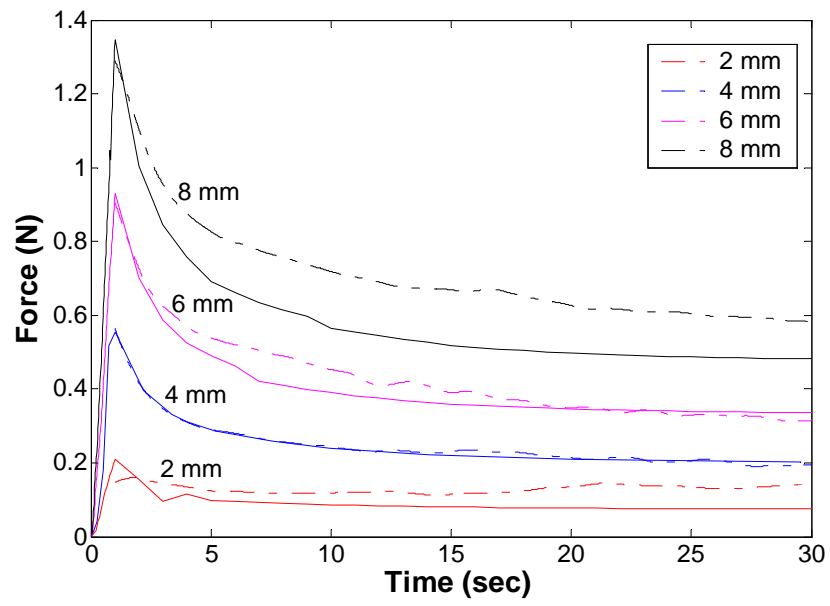
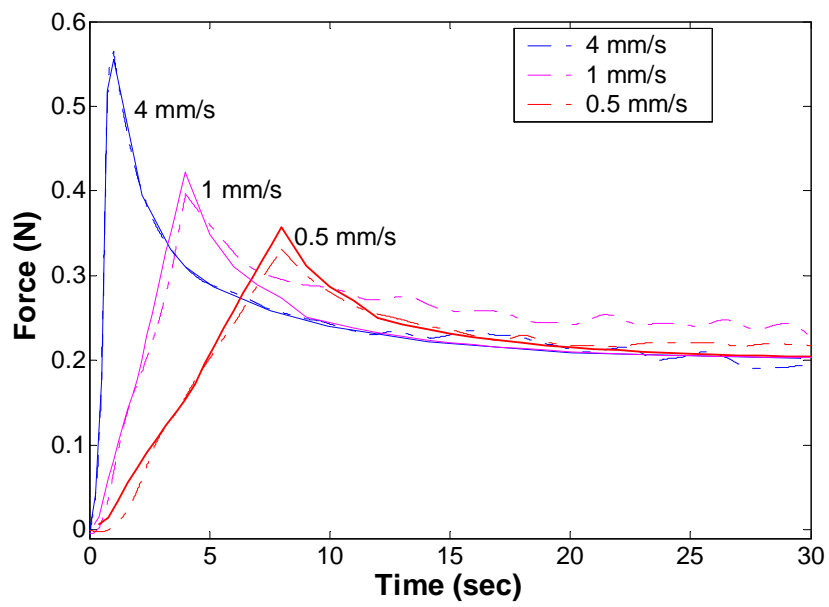


Figure 6.



(a)



(b)

Figure 7.

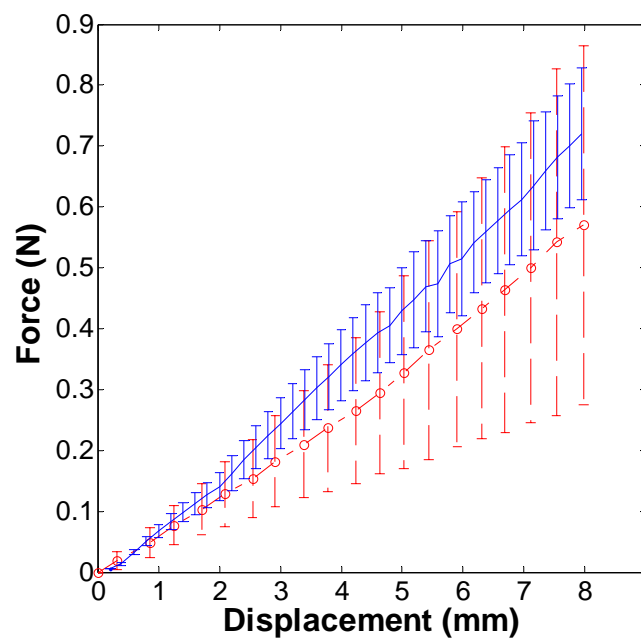


Figure 8.

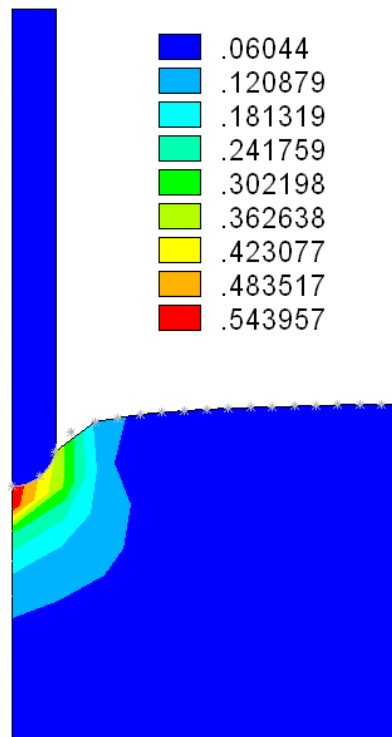


Figure 9.

Tissue Damage	Measurement Site	
	<i>in-situ</i>	<i>in-vitro</i>
Non-invasive	<ul style="list-style-type: none"> •Gao et al. •Yong-Ping and Mak •Manduca et al. •Han et al. 	
Minimally invasive	<ul style="list-style-type: none"> •Brown, et al. •Ottensmeyer •Samur, et al. •Kauer 	
Invasive	<ul style="list-style-type: none"> •Carter, et al. •Tay, et al. & Kim •Brouwer, et al. 	<ul style="list-style-type: none"> •Brouwer, et al. •Hu and Desai •Valtorta and Mazza




 Medical imaging technique
 Machine-operated electro-mechanical device
 Human-operated electro-mechanical device

Table 1.

Indentation Depth δ [mm]	Effective Young's Modulus E [kPa]
2	16.9 ± 4.9
4	12.4 ± 4.1
6	10.8 ± 4.7
8	10.0 ± 4.7

Table 2.

	Pig #1	Pig #2	Pig #3
G_1 [kPa]	2.402	3.688	0.827
G_2 [kPa]	1.733	2.495	3.333
τ_1 [s]	0.979	1.000	1.202
τ_2 [s]	5.650	9.000	10.641
G_{∞} [kPa]	4.593	3.193	5.093

Table 3.

	Pig #1		Pig #2		Pig #3	
	Initial Value	Estimated Value	Initial Value	Estimated Value	Initial Value	Estimated Value
α_1	0.275	0.309	0.393	0.429	0.089	0.388
α_2	0.199	0.243	0.266	0.256	0.360	0.098
τ_1 [s]	0.979	0.945	1.000	1.033	1.202	2.992
τ_2 [s]	5.650	7.792	9.000	6.431	10.641	11.941
C_{01} [kPa]	3.484	3.295	3.426	2.779	2.120	2.876
C_{10} [kPa]	3.484	2.563	3.426	3.459	2.120	3.240
Number of Iterations	29		18		36	
Error	3.764E-03		0.428E-03		3.462E-03	

Table 4.

Figure Captions:

Fig. 1. Our robotic indenter (a) and its components (b). The indenter is inserted into the abdominal cavity through a surgical trocar for collecting displacement and force data. The cover prevents the probe and force transducer from contacting the trocar during indentations. The numbers in the figure indicate the assembly order for sterilization purposes.

Fig. 2. A scene from the animal experiments.

Fig. 3. a) The displacement-time and force-time curves constructed from the static indentation data of pig #2 for the indentation depths varying from zero to 6 and 8 mm with a strain rate of 0.2 mm/s. b) The average force response of 3 pigs for the indentation depth changing from zero to 8 mm with a strain rate of 0.2 mm/s.

Fig. 4. a) The displacement-time and force-time curves obtained from the raw stress relaxation data of pig #2 for the indentation depths of 2, 4, 6, and 8 mm (strain rates are 2, 4, 6, and 8 mm/s respectively). b) The average force-time response of 3 pigs at the indentation depth of 4 mm (strain rate is 4 mm/s). The data points represent the mean values of three animals and the vertical bars correspond to the standard deviations over one trial per animal.

Fig. 5. The shear relaxation modulus of pig liver (pig #2) as a function of time for the different indentation depths and rates.

Fig. 6. The flow chart of the inverse finite element solution.

Fig. 7. a) The experimental force relaxation curve recorded at the indentation depths of 2, 4, 6, and 8 mm (dashed lines) and the corresponding inverse FEM solution (pig #2). b) The experimental force

relaxation curve recorded at the indentation depth of 4 mm at strain rates of 4, 1, and 0.5 mm/s (dashed lines) and the corresponding inverse FEM solution (pig #2).

Fig. 8. The experimental force-displacement response of three pigs for the indentation depth of ranging from zero to 8 mm (red dashed line) and the corresponding forward FEM solution (blue solid line).

Fig. 9. The FEM analysis shows the distribution of maximum principal strain at the indentation depth of 4 mm (pig #2). Large deformations in the soft tissue (i.e. max principal strain $\epsilon_{\max} = 0.54$) are observed around the contact region.

Table Captions:

Table 1. The classification of tissue measurement techniques.

Table 2. The effective elastic modulus of pig liver calculated for the different indentation depths.

Table 3. The coefficients of the shear relaxation function for the indentation depth of 4 mm.

Table 4. The estimated material properties of pig liver through inverse solution; α_k and τ_k are the viscoelastic coefficients and C_{01} and C_{10} are the hyperelastic coefficients. The hyperelastic coefficients given in the table correspond to the short-term response of the material. For conversion to the long-term response, they must be multiplied by $\left(1 - \sum_{k=1}^2 \alpha_k\right)$.